Characterization of Defects in ZnO Nanocrystals at Different Annealing Temperatures Using Positron Annihilation Lifetime Spectroscopy

K. R. Mahmoud

Physics Department, Faculty of Science, Kafrelsheikh University, 33516 El Geesh Street, Kafr El Sheikh, Egypt
kamalreyad@hotmail.com

The paper presents the use of positron annihilation lifetime spectroscopy (PALS) to characterize the thermally induced evolution of defects present in chemically synthesized ZnO nanoparticles using chemical bath deposition (CBD) method followed by annealing in the temperature range of 100 - 800ºC. The positron annihilation lifetime data were used to trace defect structure changes in the samples after annealing. The positron lifetime spectra were deconvoluted into three components in the annealing temperatures ranged from 400-800^{o}C, while the annealed samples at 100-300^{o}C were analyzed with four lifetime components. The calculated lifetime parameters of positron and positronium atoms allowed drawing conclusions about the degree and nature of defects of studied materials. In addition, X-ray diffraction (XRD) and scanning electron microscopy (SEM) have been performed to determine the shapes and sizes of the nanocrystalline ZnO samples. The UV- VIS Spectrophotometer was used to measure the absorbance of the synthesized ZnO nanoparticles.

1. Introduction

Zinc oxide (ZnO) is one of the semiconductor materials that are widely used in the fabrication of many photonic devices such as light emitting diodes, ultraviolet laser devices, varistors, thermoelectric devices, ……etc. It has a wide energy band gap (~3.37 eV) and high excitonic binding energy (60 meV) [1]. Therefore, the optical and electrical properties of nanostructured ZnO crystals were widely investigated by many research groups [2-4]. It is reported that the properties of ZnO strongly depend on various kinds of defects present in the ZnO nanostructure [5, 6]. Many of these structural defects such as the grain boundaries can strongly affect the electronic and optoelectronic properties of the nanostructured ZnO. Therefore, characterization of defects in nanocrystalline ZnO is very important.

Positron annihilation lifetime spectroscopy (PALS) is one of the powerful tools to characterize the various defects in a system like ZnO and can provide valuable information about the nature and abundance of these defects. It is well known that, positrons select to trap in a localized region or a vacancy defect with

very low electron density. Annihilation characteristics of positrons are consequently different in the perfect bulk state and vacancy trapped state; therefore, the identification of vacancies is very straightforward.

Recently, many researchers employed the PALS to characterize the nanocrystalline ZnO [7-11]. On the other hand, several works were published using PALS technique to study the effect of thermal treatment on the interfacial defects in ZnO nanocrystals [10-17].

In the present work, x-ray diffraction (XRD), scanning electron microscope (SEM) and positron annihilation lifetime studies on nanocrystalline ZnO are reported. The samples are prepared by Chemical Bath Deposition (CBD) method, and the structure of the ZnO nanocrystals are confirmed by x-ray diffraction analysis. Both methods provide valuable insights into defects and structure of the nanoparticles.

2. Experimental technique

2.1. Sample preparation and characterization

ZnO nanoparticles were prepared using Chemical Bath Deposition (CBD) method at 80^{o}C. Zinc nitrate hexahydrate $N_2O_6Zn6H_2O$ (Sigma–Aldrich, purity ≥ 99%) and KOH (Sigma–Aldrich, assay 85-100.5%) were selected as starting materials to prepare ZnO nanoparticles. The $N_2O_6Zn6H_2O$ was the source of the Zn^{2+}cation, and KOH acted as both a stabilizer and mineralizer. Solutions were prepared by dissolving 0.25M $N_2O_6Zn6H_2O$ and 2.135M KOH in the deionized water under magnetic stirring for 10 minutes for each one separately. Solutions are added to each other and heated at 80^{o}C in oil bath for 4 h, and naturally cooled to room temperature to obtain precipitate of ZnO nanoparticles, that are washed by deionized water several times, and dried for further characterization.

The morphology of the ZnO nanoparticles were investigated with a scanning electron microscope (SEM, JEOL JSM 6360 LA), while the crystalline structure was examined with an x-ray diffractometer (XRD, Shimadzu 6000). The absorbance of the synthesized ZnO nanoparticles were measured with UV-VIS Spectrophotometer (Shimadzu UV-2450).

2.2. Positron lifetime measurements

Positron lifetime measurements were carried out using the fast-fast coincidence ORTEC system. The specification of the system is found in reference [18]. The time resolution of the spectrometer was ~350 ps (full-width at half maximum, FWHM), measured with a ^{60}Co source at ^{22}Na energy window settings. The positron source ^{22}NaCl (10 μCi) is deposited on a 7.6 μm thick Kapton foil and sandwiched between two identical and plane faced pellets of ZnO samples. About 10^6 total counts were accumulated in each measurement.

The lifetime spectra were measured in air at room temperature. The analysis of lifetime spectra was realized by computer programme LT created by Kansy [19], with a suitable correction for the positrons annihilated in the Kapton. The lifetime spectra for the samples annealed at temperature ranges 400-800^{o}C, were decomposed into three lifetime components, a short lived (τ_1), an intermediate lived (τ_2) and a long lived (τ_3). The existence of three components is in very good agreement with positron lifetime data published on ZnO nanoparticles by other research groups [11, 17, 20, 21]. While the samples annealed at temperature ranges 100-300 ^{o}C where decomposed into four components τ_1, τ_2, τ_3 and τ_4. These components were determined by the best-fitting parameter ranged from ~1.0 to 1.2.

3. Results and Discussion:

Figure (1) shows XRD patterns of the as-synthesized ZnO nanoparticles with CBD method. It can be seen that the samples exhibit the standard wurtzite structure of zinc oxide (The observed peaks are 100,002,101,102,110,103,200, 112,201 and 202) and no impurity phase is observed. The crystallite size determined by the Debye–Sherrer equation with XRD data is found to be 50 nm.

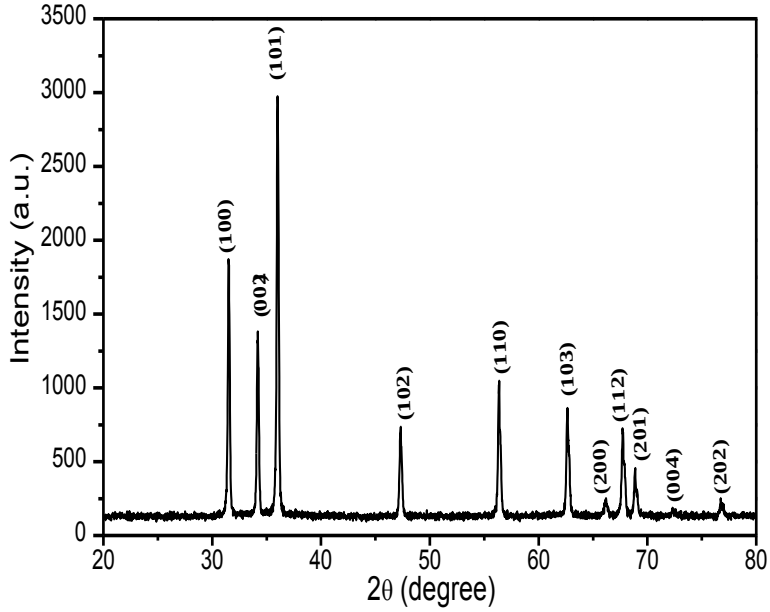

Fig. (1): X-ray diffraction patterns of ZnO nanoparticles prepared by CBD method.

Figure (2) shows the SEM image of ZnO nanoparticles prepared by CBD. The SEM image was taken at X30,000 magnification. The image shows ZnO particles are hexagonal nanorods in shape with smooth surface and the diameter of the rods is around 75-200 nm.

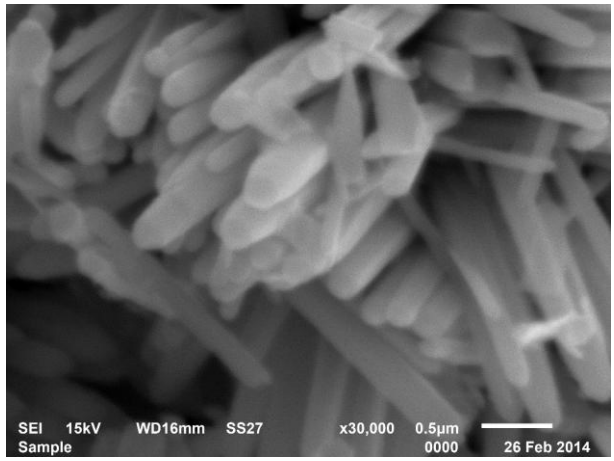

Fig. (2): Shows the SEM image of ZnO nanoparticles

Figure (3) shows the UV-Vis spectra of ZnO nanoparticles prepared with CBD method, where there is absorption edge at about 376 nm, which is the characteristic band of pure ZnO nanoparticles. This is a good evidence for the ZnO nanoparticles formation.

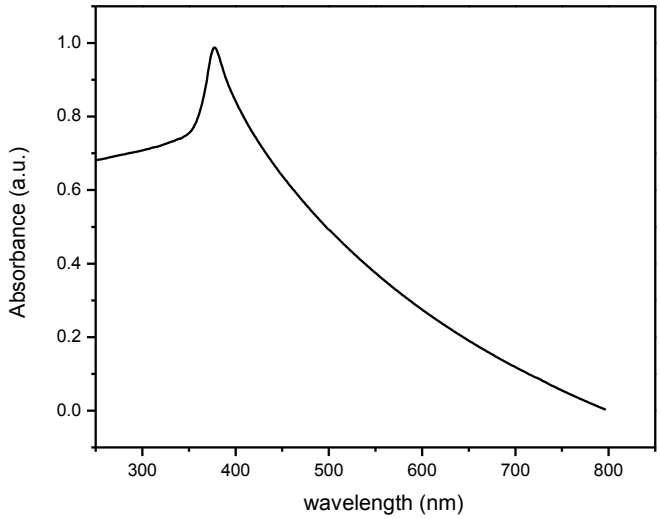

Fig. (3): UV-visible absorption spectra of ZnO nanoparticles prepared by Chemical Bath Deposition method

The positron lifetime spectra measured for the samples annealed at (100 - 300^{o}C) were fitted with four lifetime components (τ_1, τ_2, τ_3 and τ_4) with relative intensities (I_1, I_2, I_3 and I_4) respectively. While samples annealed at (400- 800^{o}C) were analyzed with only three lifetime component τ_1, τ_2 and τ_3 with relative intensities I_1, I_2 and I_3 respectively. The shortest lifetime τ_1 corresponds to annihilation of positrons at in the bulk of the ZnO. The intermediate lifetime τ_2

has been assigned to trapping of positrons at the intersection of three or more grain boundaries. The longest lifetimes τ_3 and τ_4 (τ_4 in the case of samples annealed at 100-300^{o}C) are attributed to the pick-off annihilation of ortho-positronium formed at the surface regions characterized by a large volume and low intensity. The variation of positron lifetime τ_1 and its relative intensity I_1 with annealing temperatures are shown in Fig. 4. The results indicated that, the τ_1 values are ranged from 93 – 150 ps with an average of 111.4 ± 19 ps for all the studied samples in the annealing temperature range (100 - 800^{o}C). The measured values of τ_1 are of the same order of magnitude as measured by Xiao et al [12] for bulk ZnO single crystal. At the same time, the values of τ_1 are less than the bulk lifetime of positrons (~158 ps) in ZnO reported by Chen et al [22]. However, most of references have considered the shortest lifetime (τ_1) corresponds to positron trapping in zinc vacancies (V_{Zn}) located either in the bulk and/or on the particle surface referred to as grain boundary [17, 22-24]. It is reported that the Zinc vacancies (V_{Zn}) together with oxygen vacancies (V_O) are dominant defect in ZnO [17], because they are characterized by low formation energies [25]. These kinds of defects are visible to positrons and considered strong trapping centers for them.

The results in Fig. (4), also showed that, as the annealing temperature increases from 100 to 500^{o}C, the value of τ_1 increases gradually from 105 to 150 ps due to the increase of the grain growth that influences positron annihilation centers responsible for this component. For the samples heat treated at annealing temperature larger than 500°C to 800°C, the value of τ_1 decreases to 98ps due to the thermal induced recovery of both, grain boundary and bulk located Zn vacancies. Consequently, most positrons annihilate in the bulk and/or in other kind of defects or imperfection left in the sample.

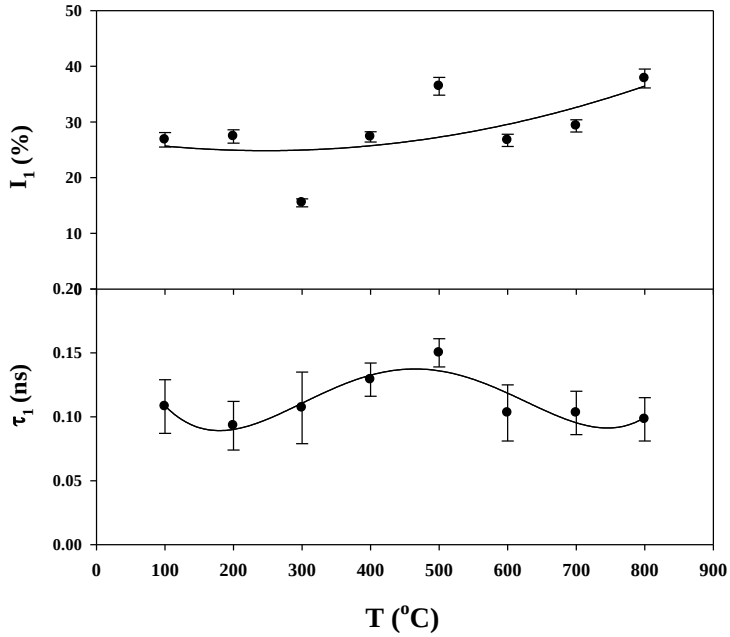

Fig. (4): Variation of positron annihilation lifetime component τ_1 and corresponding intensity I_1 with the annealing temperature of the measured samples.

The variation of the intensity of the shorter component (I_1), which is the fraction of positron annihilating at the different defect sites, as a function of the annealing temperature is shown in Fig. (4). The results indicated that, the obtained I_1 values ranged from 15.5 – 37.8% with an average of 28.4 ± 6.8% for all the studied samples in the annealing temperatures range (100 - 800^{o}C). It was also observed from Fig. (4), that the general trend of I_1 is the gradual increase in the temperature range of 100 - 800^{o}C. This means, that the fraction of positron annihilating at the different defect sites increases with increasing the annealing temperature.

The intermediate lifetime component, (τ_2) ranging from 265- 349 ps , is the positron annihilation lifetime in defect sites and/or arises from the annihilation of positrons in the Zn related large open volume vacancy complexes [23, 26]. In addition, due to the presentence of vacancy clusters located at the surface of the nanocrystal ZnO, it is prospective that positrons are mainly probing the grain boundary regions in the nanocrystalline ZnO samples because of the large positron diffusion length. This is in a good agreement with the observed lifetime results of Chakrabarti et al [16] that the surface of the nanocrystalline ZnO contains a large number of vacancy clusters and open volume Zn. Variation of positron annihilation lifetime component, τ_2, and corresponding intensity I_2 with the annealing temperatures (100-800°C) of the measured samples is shown in Fig. (5). The results indicated that the intermediate lifetime τ_2 slightly increases in the temperature range 200-500°C, which might be due to the slight increase of

the average size of vacancy cluster. After that, τ_2 showed a rapid decrease at annealing temperatures above 500°C, which indicates that the average size of vacancy cluster decreases. The relative intensity I_2 in the temperature range 100-500°C showed a little change after that, I_2 showed a little decrease at above 500°C. The reason for the reduction in I_2 can be attributed to the smaller fraction of positrons annihilating at the surface and the interface region because of grain growth. While, the decreasing in τ_2 probably reveals recovery of the vacancy clusters, which begin to collapse and cause shrinking of the vacancy clusters.

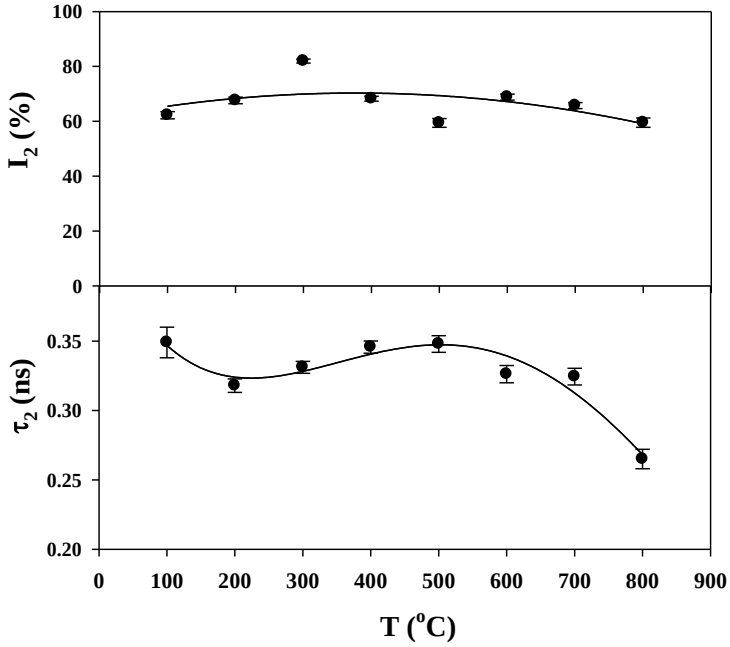

Fig. (5): Variation of positron annihilation lifetime component τ_2 and corresponding intensity I_2 with the annealing temperature of the measured samples.

According to the most popular hypothesis, the longest lifetime components (τ_3 and τ_4) are attributed to the pick-off annihilation of ortho-positronium formed in the inter-crystalline regions characterized by a large volumes [11, 17]. In our case, this corresponds to the very long lifetime components τ_4 (4.6±0.6, 9.9±0.8 and 6.6±0.70) ns with relative intensity I_4 (0.91±0.14, 0.7±0.17 and 0.36±0.06)% for the samples annealed at temperature 100, 200 and 300°C respectively. The very weak intensity of this long lifetime component originates from the formation of positroniums at the sample surface and can be neglected. The most important component is the long lifetime τ_3. Fig. (6), shows the variation of τ_3 and corresponding intensity I_3 with the annealing temperature ranged from 100-800°C. It is clear from Fig. (6), that τ_3 dramatically increases from 1.2±0.22 ns to 5±0.28 ns when the annealing temperature increases from 100 to 600°C, after that τ_3 decreases at higher annealing temperatures. The decrease of τ_3 may be due

to the reduction of inter-crystalline free volume concentration due to the thermally induced agglomeration of grains in the samples. The results in Fig. (6), also showed that the relative intensity I_3 decreases very fast from 10.13±0.9 % at annealing temperature 100°C to 1.4±0.02 % at annealing temperature 400°C. A similar behavior was also shown in the data reported by Karbowski et al [27], and is to be attributed to the sintering process. The relative intensity I_3 does not change noticeably and nearly constant at temperature above 400°C.

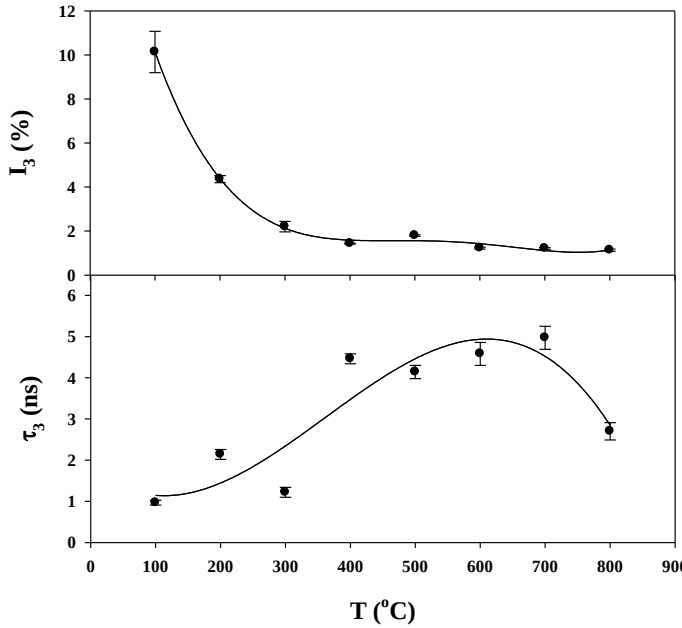

Fig. (6): Variation of the longest lifetime component τ_3 and corresponding intensity I_3 with the annealing temperature of the measured samples.

The variation of the overall defect (vacancy) concentration in the samples can be understood from the variation of the mean positron lifetime, which is defined as:

$$\tau_{av} = (I_1\tau_1 + I_2\tau_2 + I_3\tau_1)/(I_1+I_2+I_3)$$

Figure (7), shows the variations of the average positron lifetime (τ_{av}) as a function of annealing temperature of the measured samples. The value of τ_{av} shows a systematic decrease trend as the annealing temperature increases. This clearly indicates a gradual reduction of overall defect concentration in the samples with increasing the annealing temperature. However, the calculated values of τ_{av} ranged from 0.22 to 0.4ns which are quite high than the bulk lifetime of positron in ZnO (158 ps) [22], which confirm the presence of large vacancies in the samples.

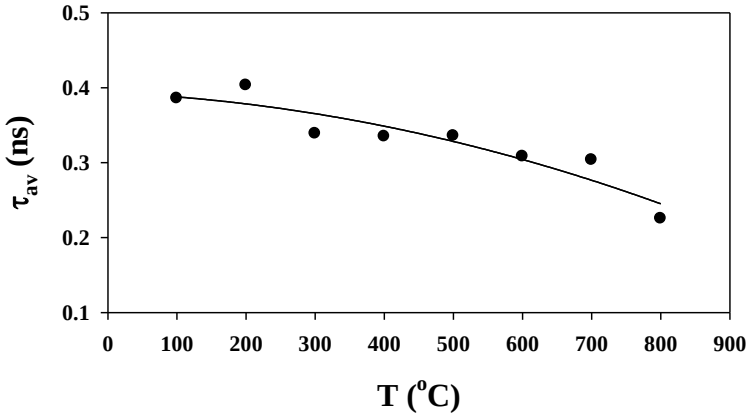

Fig. (7): Variations of the average positron lifetime (τav) with the annealing temperature of the measured samples.

4. Conclusion

Samples of ZnO nanoparticles were synthesized by chemical bath deposition (CBD) method, then annealed at different temperatures in the range of 100–800°C, were studied by X-ray diffraction, SEM, UV and positron lifetime annihilation technique. Positron annihilation lifetime studies revealed significant changes in properties of ZnO nanoparticles with annealing temperatures and indicated the presence of vacancy defects at the surface of these nanocrystaline ZnO. The crystal quality of the ZnO nanocrystals were investigated by x-ray diffraction (XRD) technique and showed that the ZnO particles are hexagonal nanorods in shape with smooth surface and the diameter of the rods around 75-200 nm. The UV-Vis spectra of ZnO nanoparticles has an absorption edge at about 376 nm, which is the characteristic band of pure ZnO nanoparticles. The positron annihilation lifetime results revealed that there are two long lifetimes components (τ_3 and τ_4) which are attributed to the pick-off annihilation of ortho-positronium formed in the inter-crystalline regions and surface regions respectively.

The variation of the average positron lifetime (τ_{av}) as a function of annealing temperature showed a systematic decreasing trend as the annealing temperature increases, which clearly indicates a gradual reduction of overall defect concentration in the samples with increasing the annealing temperatures.

References

1. Z. L. Wang, *J. Phys.: Condens. Matter* **16**, R829 (2004).
2. A. B. Djurisic and Y. H. Leung, *Small* **2** (8-9) 944 (2006)
3. A. B. Djurisic, A. M. C. Ng and X. Y. Chen, *Prog Quant Electron* **34**, 191(2010).
4. A. Janotti and C.G. Van de Walle, *Rep. Prog. Phys.*, **72**, 126501 (2009).

5. S. Dutta, S. Chattopadhyay, A. Sarkar, M. Chakrabarti, D. Sanyal and D. Jana, *Prog Mater Sci*, **54**, 89 (2009).
6. A. Sundaresan, R. Bhargavi, N. Rangarajan, U. Siddesh and C. N. R. Rao, *Phys Rev B*, **74**, 161306 (R) (2006).
7. F. Tuomisto, V. Ranki, K. Saarinen and D. C. Look, *Phys Rev Lett*, **91**, 205502 (2003).
8. Z. Q. Chen, M. Maekawa, S. Yamamoto, A. Kawasuso, X. L. Yuan, T. Sekiguchi, R. Suzuki, and T. Ohdaira, *Phys. Rev. B* **69**, 035210 (2004).
9. G. Brauer, W. Anwand, D. Grambole, J. Grenzer, W. Skorupa, J. Cizek, J. Kuriplach, I. Prochazka, C. C. Ling, C. K. So, D. Schulz and D. Klimm, *Phys Rev B* **79**, 115212 (2009).
10. A. Zubiaga, F. Plazaola, J. A. Garcia, F. Tuomisto, V. Munoz-Sanjose and R. Tena-Zaera, *Phys Rev B* **76**, 085202 (2007).
11. D. Wang, Z. Q. Chen, D. D. Wang, N. Qui, J. Gong, C. Y. Cao and Z. Tang, *J Appl Phys*, **107**, 023524 (2010).
12. P. C. Xiao, W. Ke-Fan, Z. Yang, G. Feng-Li, W. Hui-Min and Y. Bang-Jiao, *Chinese Physics B*, **18** (5), 2072 (2009).
13. Z. Q. Chen, M. Maekawa, A. Kawasuso, S. Sakai and Naramoto, *Physica B* **376-377**, 722 (2006).
14. R. Ono, T. Togimitsu and W. Sato W., *J Radioanal Nucl Chem* **303**, 1223 (2015).
15. S. Dutta, M. Chakrabarti, S. Chattopadhyay, D. Jana, D. Sanyal and A. Sarkar, *J Appl. Phys.* **98**, 053513-1 (2005).
16. M. Chakrabarti, D. Jana and D. Sanyal, *Vacuum* **87**, 16 (2013).
17. A. K. Mishra, S. K. Chaudhuri, S. Mukherjee, A. Priyam, A. Saha and D. Das, *J Appl Phys* **102**, 103514 (2007).
18. K. R. Mahmoud, S. Al-Sigeny, T. Sharshar and H. El-Hamshary, *Radiat. Phys. Chem.* **75**, 590 (2006)
19. J. Kansy, *Nucl. Instrum. Methods A* **374**, 235 (1996).
20. A. Roychowdhury, S. P. Pati, A. K. Mishra, S. Kumar and D. Das, *J Phys. Chem. Sol.* **74**, 811(2013)
21. S. K. Sharma, P.K. Pujari, K. Sudarshan, D. Dutta, M. Mahapatra, S. V. Godbole, O. D. Jayakumar and A. K. Tyagi, *Solid State Commun* **149**, 550 (2009).
22. [22] Z. Q. Chen, S. Yamamoto, M. Maekawa, A. Kawasuso, X. L. Yuan and T. Sekiguchi, *J Appl Phys* **94**, 4807 (2003).
23. G. Brauer, J. Kuriplach, J. Cizek, W. Anwand, O. Melikhova, I. Prochazka and W. Skorupa, *Vacuum* **81**, 1314 (2007).
24. D. Wang, Z. Q. Chen, D. D. Wang, N. Qi, J. Gong, C. Y. Cao and Z. Tang, *J Appl Phys* **107**, 023524 (2010).
25. A. Janotti and C. G. Van de Walle, *Phys Rev B* **76**, 165202 (2007).
26. Z. Q. Chen, M. Maekawa, S. Yamamoto, A. Kawasuso, X. L. Yuan, T. Sekiguchi, R. Suzuki, and T. Ohdaira, *Phys. Rev. B* **69**, 035210 (2004).
27. A. Karbowski, K. Fedus, J. Patyk, L. Bujak, K. Służewski and G. Karwasz *NUKLEONIKA*, **58**(1), 189 (2013).